Textures and Microstructures, 1996, Vol. 26–27, pp. 231–243
Reprints available directly from the publisher.
Photocopying permitted by license only

THE NATURE OF TEXTURE COMPONENT DEVELOPMENT IN BCC SINGLE CRYSTALS

S. V. DIVINSKI and V. N. DNIEPRENKO

Institute of Metal Physics, National Academy of Sciences, Vernadsky str., 36, Kiev-142, 252142, Ukraine

(Received 10 September 1995)

Textural changes occurring in deformed BCC single crystals of (001)[110], (001)[100], and (110)[001] orientations have been studied by simulation of plastic deformation. It was shown that a correlation between microstructure and texture must be taken into account to interpret existing experimental data. Rolling of (001)[100] single crystals give rise to two microstructure types that correspond to different texture components, {001}<100> and {001}<230>, with the first component accommodating a transition in orientations between two symmetrical positions of second component. Suggestion that such a behaviour must be widely observed in other unstable orientations has been put forward. For example, if a (110)[001]-oriented crystal does not undergo mechanical twinning and its rolling texture can be presented as a sum of two components {112}<111> and {110}<001>, we must also expect the presence of two corresponding structure types. Disclination mechanisms of formation of the transition structure-textural components have been considered.

KEY WORDS: Texture, computer simulation, single crystal, plastic deformation, microband, disclinations

INTRODUCTION

Dislocation microstructures must be studied along with textural investigations for comprehensive understanding of processes occurring at plastic deformation. Such types of experiments have been carried out by a number of researches who observed fascinating features that furnished insights into the nature of development of axial and rolling textures in FCC and BCC metals. Hu (1962, 1963) and Walter *et al.* (1962, 1965) pioneered the concurrent use of textural analysis and electron microscopy investigation. Their results suggest that formation of a one-component texture, such as in the *Si*-iron (001)[110] single crystals under rolling, is accompanied by development of a homogeneous dislocation structure. In the case of a (001)[100] single crystal subjected to plane deformation the texture (001)<230> was shown to be formed. Two sub-structure components correspond to this texture. These electron-microscopy data allowed the authors to give a new interpretation of mechanisms of texture formation.

Vandermeer and McHarque were first who showed that each texture component in extruded *Al* is featured by a specific microstructure, Vandermeer *et al.* (1964). The same behaviour was earlier observed by Hu (1962) and by Walter *et al.* (1962) for the (001)[100]-oriented crystals, but they did not attribute the different type of

Dedicated to memory of Prof. Hsun Hu.

microstructure to different texture components. Later, the different microstructures of grains oriented differently has been demonstrated for BCC polycrystals, Trefilov *et al.* (1975). Next step was done in a set of papers where a general agreement between dislocation structures and texture components was established, Dnieprenko *et al.* (1982); Dnieprenko (1983). Furthermore, each type of dislocation microstructure was found to be formed as a result of action of different microscopic mechanisms of slip.

In some cases such analysis of micro-mechanisms of plastic deformation by electron-microscopic data may be strongly prohibited owing to ambiguous interpretation of orientations of slip planes. Therefore, it can be difficult to attribute the formation of a texture component to action of a specific set of dislocation slip systems. In view of this it was suggested to complete the electron-microscopical and textural investigations by computer simulation to analyse the specific micro-mechanisms, Divinski *et al.* (1993, 1994). Such combined analysis has allowed to clarify the problems of ambiguous interpretation of the electron-microscopy results.

Unfortunately, a polycrystal is a system with a huge number of not easily evaluated parameters, such as grain boundary effect, intergranular interaction and many others. From a physical point of view the experiments on single crystals concern of systems with a substantially lower number of free parameters. Thus, the study of plastic deformation in single crystals may be more appropriate and may give the crucial information about the initial orientation effect on a choice of particular dislocation mechanisms. This was the main object of the present paper.

DESCRIPTION OF MODELS

In this work the simulation of texture formation under plastic deformation was carried out within the model that is intermediate between the approaches of Sachs and Taylor, Divinski *et al.* (1993). Dislocations were allowed to slip mainly on {110} and {112} types of planes. Slips on other plane types, for example on the {123} planes, can be presented as some combinations of slips in the above mentioned main systems and they were not taken into account in an explicit form.

Only one, maximally loaded, slip system was chosen at each elementary step of the plastic deformation. It was the slip system that was active. This approach was the most comprehensively developed by Leffers (1968a, 1968b). Nevertheless, only the final distribution of deformed grains on orientations was compared with an experiment in these papers. In such a case it is difficult to suggest a method for rigorous splitting of the total texture on different components by some physical ground.

However, to do this we will monitor the active slip system on each elementary step of plastic deformation specially marking all crystallographically different slip systems, Divinski *et al.* (1993). Loading of the kth slip system will be determined in agreement with the value of the Schmid factor, Divinski *et al.* (1993). The stress tensor corresponds to tension in the rolling direction (RD) and to equivalent compression in the normal direction – ND perpendicular to the rolling plane.

To incorporate in the model the different types of slip systems a concept of threshold shear stresses must be taken into account and a possibility v of slip system activation is to be introduced. General agreement with experiments on BCC polycrystals is achieved if we adopt the following values: $v_{\{110\}}=0.9$, $v_{\{112\}}=1.0$, Divinski *et al.* (1994). Simulation of plastic deformation in polycrystals, Divinski *et al.* (1993, 1994) shows that if to monitor the crystallographic indices of active slip system on each elementary step of

plastic deformation, then we may see that beginning with some deformation stage (typical 20–30%) the alternative slipping is developed. Owing to an infinitesimal strain on each elementary step and high enough frequency of change of acting slip system this fact may be treated as a simultaneous activation of several (two or three, sometimes more) slip systems. Thus, an arbitrary texture may be presented in a form clearly distinguishing the texture components on specific ways of plastic deformation. Namely, let us mark the grain orientations by special symbols in dependence on the slip system types which acted on the last deformation stages, Δ – $\{110\}\langle 1\bar{1}1\rangle+\{112\}\langle 11\bar{1}\rangle$; ° – $\{112\}\langle 11\bar{1}\rangle$; • – $\{112\}\langle 11\bar{1}\rangle$ + $\{112\}\langle 11\bar{1}\rangle$. Here, for convenience sake, we mark the alternative action of two slip system types (which differ crystallographically) *A* and *B* as *A+B*. Similarly, the alternative action of a number of slip systems of the same type, say *A*, is marked as *A+A*. And, finally, if only one slip system was activated we use the only corresponding symbol (e.g. *A*). To present the grain orientations we study the last 25 elementary deformation steps and we use the corresponding symbols in dependence on a set of activated slip systems.

Single crystals were simulated as *quasi-single-crystals* with small, about 5°, dispersion of subgrain orientations around the initial orientation. Such an approach is legitimate because some texture dispersion is always formed during plastic deformation of single crystals as a result of strain-stress heterogeneity through the crystal. Thus, the subsequent deformation will deal with a "polycrystal" and consideration of the sample as a single crystal will be not correct.

In the ODF simulation we used the general approach of limited fibre components, Dnieprenko *et al.* (1993) that allowed to include also the anisotropic spreads of texture maxima. Within this model the dispersion of grains orientations for a given component must be described in some local co-ordinate system that is related to the texture axis of the component:

$$f(g_\gamma) = A \exp\left\{\frac{\gamma_2^2}{2\sigma_1^2}\right\} \bullet \exp\left\{-\frac{1}{2}\left(\frac{|\gamma_1+\gamma_3| - \sigma_3 + |\sigma_3 - |\gamma_1+\gamma_3||}{2\sigma_2}\right)^2\right\}, \quad (1)$$

The set of Eulcrian angles $g_\gamma = (\gamma_1, \gamma_2, \gamma_3)$ defines the grain orientation with respect to the local coordinate system introduced above; σ_1, σ_2, and σ_3 are the distribution parameters. It is noteworthy that such ODFs of different texture components are described in different local coordinate systems which are differently oriented with respect to the sample coordinate system and which are related to specific positions of texture axes of these components. To calculate the ODF in a sample coordinate system the special relations must be used, Dnieprenko *et al.* (1993).

PLASTIC DEFORMATION OF SINGLE CRYSTALS

Let us consider the mechanisms of plastic deformation in single crystals of various orientations.

(001)[110] orientation. Rolling of BCC single crystal with this orientation is known to do not result in any significant transformation of the initial orientation, it stays stable up to a high strain (Figure 1a). From this point of view the dislocation structure of rolled b.c.c. single crystals with the (001)[110] orientation has a prominent interest.

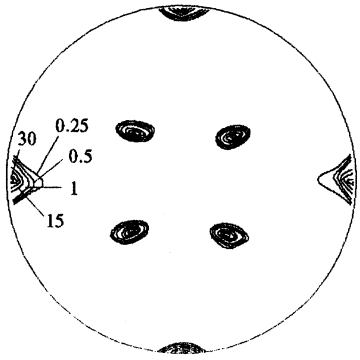

(a)

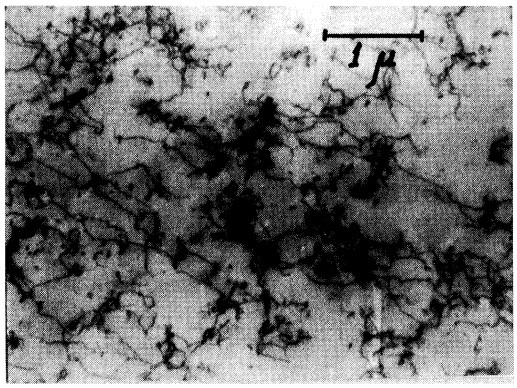

(b)

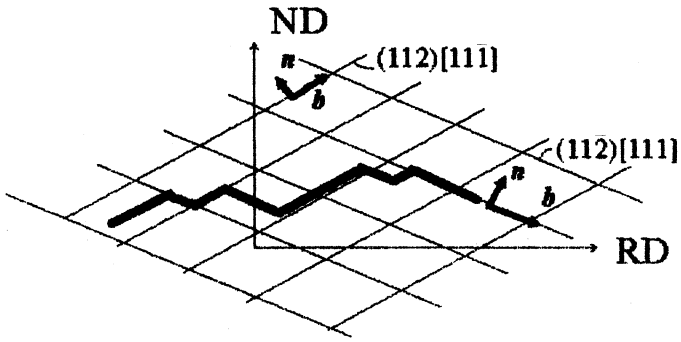

(c)

Figure 1 Texture and microstructure of a *Mo* (001)[110] single crystal deformed by rolling. (a) pole figure {110}, ε=80%. (b) dislocation structure. (c) a scheme of dislocation slips in the plane perpendicular to TD. Here *n* and *b* are the normal to slip plane and the Burgers vector of the dislocations.

In this case no cellular dislocation structure is formed (Figure 1b). Unfortunately, unambiguous determination of the activated slip systems is not possible by the external view of such dislocation structure. If a cellular dislocation structure is formed, the analysis of activated slip systems can be carried out by Takeuchi's model, Takeuchi (1970, 1980). Otherwise, the texture simulation may be used to establish the slip systems that ran during plastic deformation. The simulation shows that deformation is carried out by the alternative slip of dislocations in two systems : $(112)[11\bar{1}]$ and $(11\bar{2})[111]$ and it does produce practically no dispersion of the initial orientation. Note that the Burgers vectors of the dislocations and normals to the slip planes lie in the same plane formed by RD and ND, see Figure 1c. This is the reason to the fact that the dislocation structure in the rolling plane consists of randomly distributed dislocation segments and its forms no regular pile-ups of dislocations (since lines of transactions of the slip planes are perpendicular to RD). In this case, the dislocation distribution in the plane perpendicular to the transversal direction (TD) is likely to be, at least, more regular.

(001)[100] orientation. Two microstructure components are generally observed in the deformed state, Hu (1962); Walter *et al.* (1962). Thus, in view of above mentioned correlation between texture and microstructure the texture must be composed of two components that differ crystallographically (which are not connected by symmetry relations). Analysis of experimental pole figures (Figure 2a). within the approach of limited fibre components shows that this pole density can really be decomposed as a sum of two components, namely of {001}<230> and {001}<100>, see Figure 2b and Table 1. Note that we refer two preferred orientations (001)[230] and (001)[$\bar{2}$30] as the same texture component {001}<230>. The texture axes of the {001}<230> component are deflected from RD to TD by an angle of about 34 degrees. The precise position, as was pointed out by Hu (1962), depends on current strain. The dispersion of the second component is more anisotropic with the texture axis at the center of the {001} pole figure.

Preliminary simulation of texture formation at plastic deformation shows that the displacement of the maxima of pole density from (001)[100] to (001)[$\bar{2}$30] (or to (001)[230]) does depend on the strain, but orientations near initial orientation (001)[100] disappear even at moderate strains (Figure 2c). This obviously contradicts the experiment.

The component of microstructure with near-random dislocation distribution (Figure 2e) correspond to the {001}<230> texture component. A second structure component is characterized by microbands with a wide spread of orientations, Figure 2e, according to Hu (1962; 1963). This component accommodates total transition in orientations between two symmetric orientations of the main component {001}<230>. A conventional example of such transition is presented in Figure 2f.

The simulation reveals mainly two deformation modes : (*i*) $\{112\}\langle 11\bar{1}\rangle$ + $\{112\}\langle 11\bar{1}\rangle$ and (*ii*) $\{112\}\langle 11\bar{1}\rangle$ + $\{110\}\langle 1\bar{1}1\rangle$. The ratio of volume fractions of these two modes depends on the current strain. At low strain only the second mode is active. The contribution of mode (*i*) increases with strain and it becomes the most pronounced at high strains. In the present model the texture component {001}<100> is observed only at the initial stages of deformation, and plastic deformation proceeds through dislocation slip by mode (*ii*). Since experimentally this component stays at high strains, too, we may conclude that some assumptions of the Sachs model are not valid in this case. Let us in detail consider the mechanisms of lattice rotation during plastic deformation. Let E_+ and E_- be the symmetric and anti-symmetric components of the

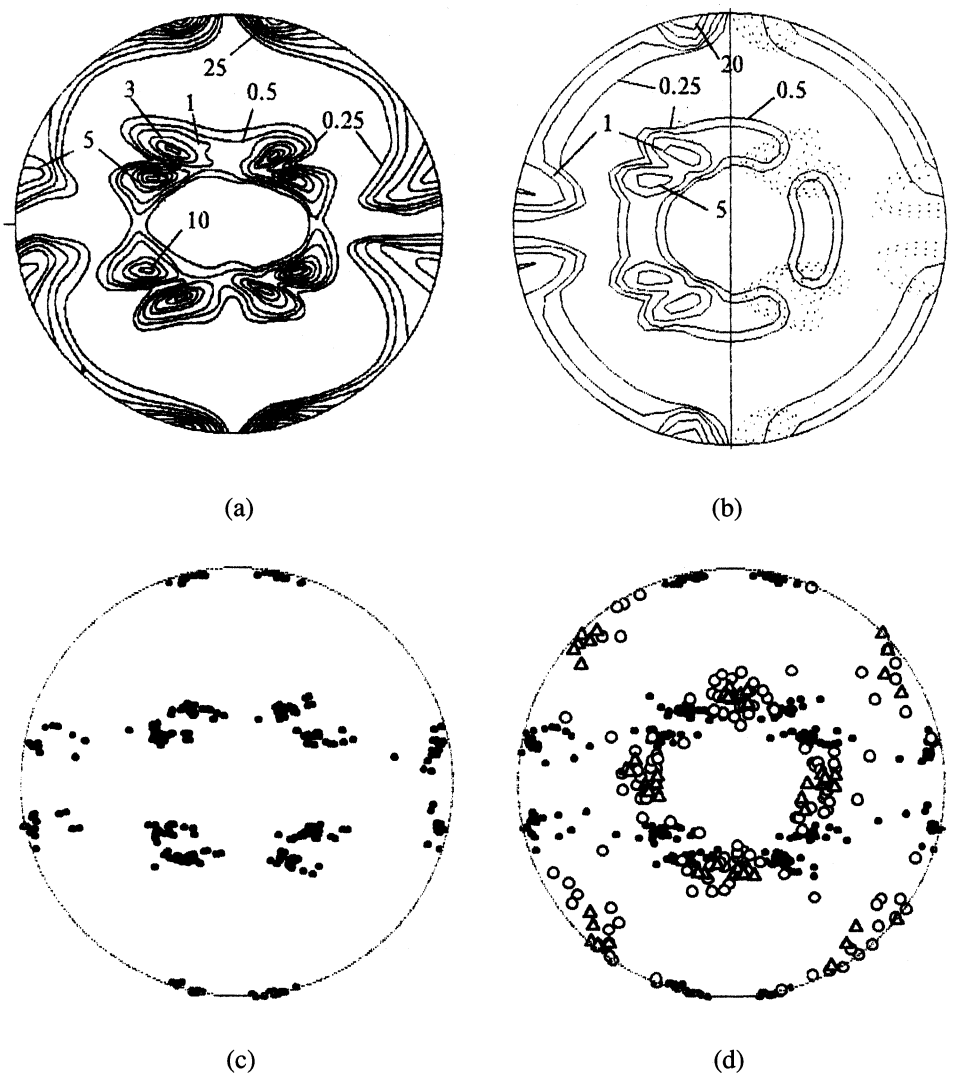

Figure 2 Texture and microstructure of an *Fe-Si* (001)[100] single crystal deformed by rolling. (a) pole figure {110}, ε=80%. After Hu (1963). (b) decomposition of pole density on separate components {001}<100> (——) and {001}<230> (.....) (right) and the total model pole density (left). (c) model pole figure calculated by a standard technique ε=70%. (d) model pole figure calculated with allowance for disclinational presentations about sub-crystal re-orientations. ε=70%.

(e)

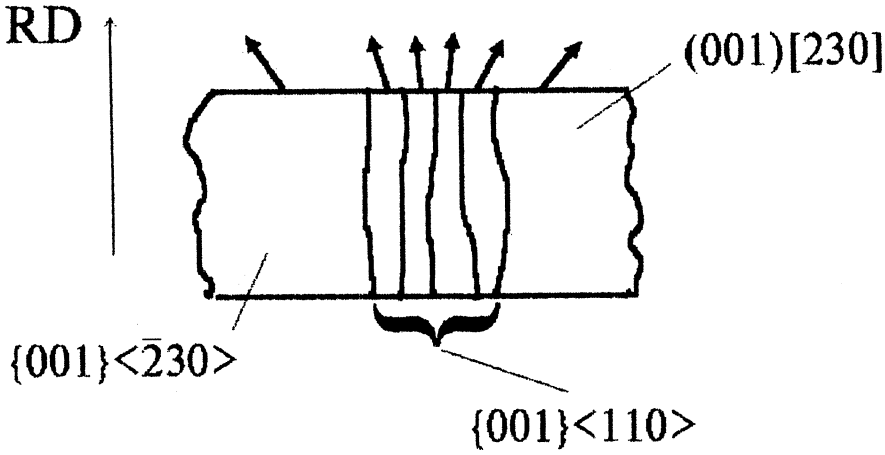

(f)

Figure 2 Texture and microstructure of an *Fe-Si* (001)[110] single crystal deformed by rolling. (e) dislocation structure. After Hu (1962). (f) a model for structure formation and for development of misorientation between symmetric orientations (001)[230] and (001)[230]. Local directions of the (100) vectors are pointed by arrows.

Table 1 Component composition of model texture for the (001)[100]-oriented crystal. V_k is the volume fraction of the kth component.

k	*preferred orientation* (hkl)	[uvw]	*texture axis*	V_k	σ_1	σ_2 *degrees*	σ_3
1	(001)	[100]	| 001 |	0.3	8.	10.	25.
2	(001)	[230]	| 110 |	0.7	4.	9.	6.
	(001)	[$\bar{2}$30]	| $\bar{1}$10 |				

strain tensor for a given grain. While the first component is responsible for the change of grain shape, the second one gives rise to rotation of the grain. In this case the change of grain orientation depends on conditions on the grain boundaries. More often than not, the absolutely rigid boundary conditions are adopted. Thus, resulting rotation Ω of grain lattice is calculated by:

$$\Omega = -E_{-} . \tag{2}$$

As it follows from the above, in case of formation of microbands with orientations near (001)[100] equation (2) is most likely to fail. We propose to use the following relation instead of (2):

$$\Omega = -\alpha \cdot E_{-} . \tag{3}$$

where conditions on boundaries are taken into account by a factor α.

Hence, our model was extended as follows. Deformation starts with α=1 for all sub-crystals. In the deformation scheme we introduce phenomenological the probability of formation of microbands as a result of dislocation slips. If a microband is formed, the re-orientation of its volume follows relation (3) with α=0. This allows to reach a general agreement with the experiment, see Figure 2d.

From our point of view, the difference between conditions at boundary from crystal side and microband side lies in loss of coherent relations between the lattices in last case. Unlike to ordinary boundaries that can be considered within dislocation presentations, such boundaries are to be viewed by disclination presentations. In view of this, one more justification can be found for relation (3). Indeed, in approximation of ideal accommodation at boundaries, the matrix of rotation of a crystal region near a boundary with normal N is, Zolotarevsky *et al.* (1989):

$$\Delta\omega_N = \frac{1}{b} \sum_{p=1}^{M} \Delta\gamma_p \left\{ N \cdot b_p \left(N \times n_p \right) - \lambda \left\{ \left(N \times n_p \right) \cdot b_p \right] N \right\}, \tag{4}$$

where $\Delta\gamma_p$, b_p, and n_p are the increment of slip, the Burgers vector, and the normal to the slip plane for the p th slip system, respectively; λ is a parameter of accommodation. The parameter allows for additional slip occurring at a boundary with singularity in dislocation distribution, Zolotarevsky *et al.* (1989). Relation (4) has been

derived within presentations that re-orientation of crystal fragments proceeds by formation of partial disclinations at the boundaries. For interior parts of crystal fragments we must average the relation (4) over different orientations N of the boundary segments. As a result, a relationship similar to the Taylor one can be obtained. On the other hand, if we apply this relation to interior parts of microbands, the result will be drastically distinguished from the above. Indeed, now, the orientation of the normal to the microband boundary coincides with the normal to the slip planes. Thus $N \times n_p = 0$ and $\Delta\omega_N = 0$ similar to Eq. (3) Deviation of N from n_p can be taken into account by the factor α in Eq. (3).

(110)[001] orientation. According to Dunn (1954) the deformation texture after rolling to 70% reduction looks like that presented in Figure 3a. The texture can be described as a sum of two components, namely {001}<110> and {111}<112>. The last includes two symmetric sub-components. Simulation of plastic deformation within a standard model can only explain the formation of the {111}<112> component. In this case, the dispersion of the maxima is rather isotropic and there is no transition region between them, see Figure 3b. However, such transition density is clearly observed in the experiment, see Figure 3a. The {001}<110> weak component in the experiment was suggested to be derived from mechanical twins formed in early stages of deformation, Dunn (1954). Since mechanical twinning is not a general feature of all BCC metals, we omit it in out model. As it was shown above by interpretation of the Hu's results on the (001)[100] orientation, the misorientation between two symmetric orientations is to be formed via specific structure-texture elements, say, by microbands. Hence, the misorientation between (111)[$\bar{1}\bar{1}$2] and (111)[11$\bar{2}$] can be formed via development of some other transition components. These may be either microbands or something else. Textural and microstructural changes occurring in deformed molybdenum crystals oriented for (110)[001] plain strain compression have been studied by X-ray pole figures and transmission electron microscopy, Carpay *et al.* (1977). Our model of Figure 3b agrees with their results. In such a case the volume fraction of the transition component is likely to be moderately low and attention was not drawn to the problem of its detection. Unfortunately, from the experiment of Carpay *et al.* (1977) it is not clear how the re-orientation of different regions of the crystal have been performed. Subsequent experimental investigations are necessary to clarify this problems.

If we adopt the assumptions that have been made above for the (001)[100] orientation, the model pole figure, Figure 3c, will be in better agreement with the experiment, Figure 3a (excluding orientation that can easily be obtained in the model by incorporating the possibility of mechanical twinning).

Within the suggested framework we may re-consider the data of Carpay *et al.* (1977) concerning deformed *Mo* crystals with (001)[100] orientation, where the initial orientation was not split into two symmetric components. Presented experimental data of electron microscopy do not reveal a presence of any microband. Thus, in view of absent of any structure element that may accommodate the misorientation, one would not accept a split of the initial orientation. Such stability of the (001)[100]-oriented *Mo* crystals under rolling needs further experimental and theoretical investigations.

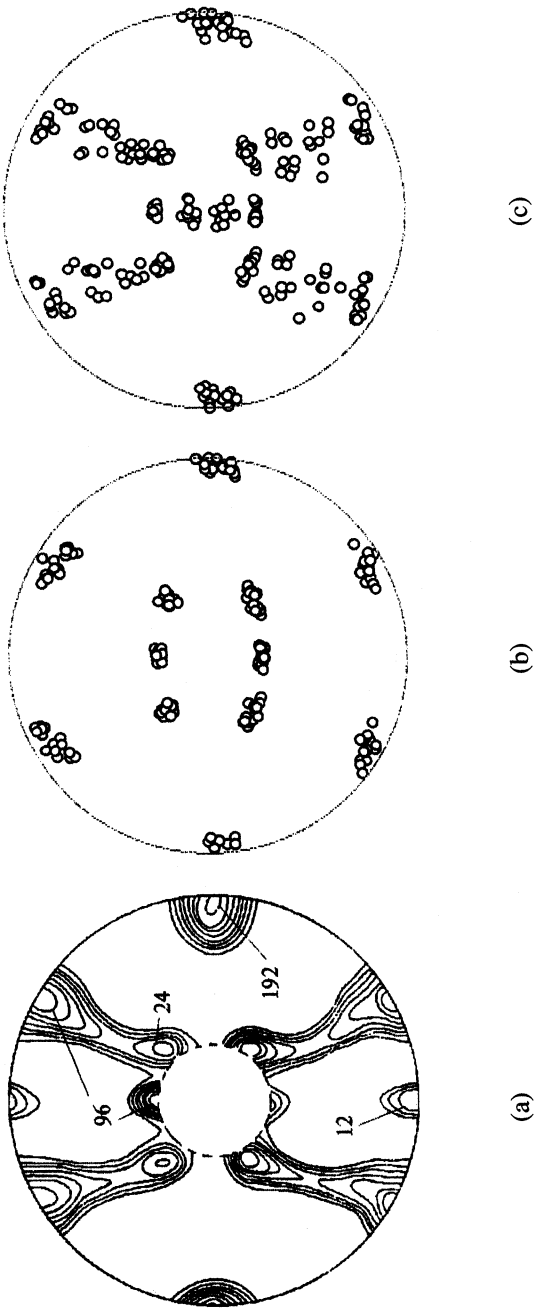

Figure 3 Texture and microstructure of a *Mo* (110)[001] single crystal deformed by rolling. (a) pole figure {110}, ε=70%. After Dunn (1954). (b) model pole figure calculated by a standard technique ε=70%. (c) model pole figure calculated allowance for the disclinational presentations about sub-crystal re-orientations. ε=70%.

DISCUSSION

Dislocation density is known to grow with strain. These dislocations produce extended fields of elastic forces. Thus, appearance of collective or self-organisation effects may be expected at high dislocation density, especially if there is a predominance of dislocations with the same sign. Then, the system acquires qualitatively new features. In dependence on relative arrangement of the dislocations the total free energy may reach a level allowing the spontaneous relaxation processes. After such relaxation, the further storing of the free energy may take place again up to reaching of a new relaxation level.

Rotational deformation, *i.e.* change of sample shape as a result of rotation of extended regions of material, may be one of such relaxation modes in a material, in which the predominance of dislocations with the same sign was previously formed. They are partial disclinations that are responsible for such rotations, De Wit (1972). Unlike dislocations that describe translational singularities, the disclinations present angular singularities that appear at passing along a contour confining the boundary of rotated materials.

Li *et al.* (1970) pioneered the use of disclinational presentations for description of plastic deformation of polymers. In case of crystalline materials, the disclinations were widely used by Romanov *et al.* (1983) and Rybin (1986).

The analysis shows that $(112)[11\bar{1}]$ and $(11\bar{2})[111]$ are the slip systems in the case of deformation of (001)[110] crystal. These systems are symmetric with respect to the rolling plane and have non-codirected Burgers vectors. Therefore, formation of some predominance of dislocations with the same sign is generally prohibited, whereas a condition $\Delta\rho=\rho_+-\rho_->>1$ is a necessary condition for the appearance of rotational instability, Vladimirov *et al.* (1986). Here ρ_+ and ρ_- are the dislocation densities of dislocations with opposite signs. Hence, no self-organization phenomenon is observed at deformation of crystals with this orientation. Dislocation structure remains random and neither cell structure nor microbands are formed.

Unlike the stable orientation (001)[110], the following slip systems are running at initial deformation stages of the (001)[100] single crystals: $(101)[\bar{1}11]$, $(101)[\bar{1}\bar{1}1]$, $(\bar{1}01)$ [111], and $(\bar{1}01)[1\bar{1}1]$. Since some spread of the initial orientation will be formed for any of several reasons, the orientation of a given region of the crystal will differ from initial. Then, only two slip systems will remain active and they will further rotate the crystal out of the initial orientation. Then the crystal orientation changes to that with equal threshold of shear stresses in (110) and (112) planes, the proper slip systems from the {112}<111> family will act also. Coincidence of Burgers vectors of running dislocations is crucial, although slipping proceeds alternatively on different planes: passing from (110) to (112) and *vice versa*. This causes the formation of predominance of dislocations with the same sign that is a necessary condition for development of rotational deformation modes. As a result, microbands are abundantly developed.

Processes of deformational instability occur even at low strains, although, as a rule, they are experimentally observed at higher strains. This is caused by the fact that the density of self-organization elements at initial deformation stages is relatively low and, thus, the probability of their encountering is inadequate for routine techniques of the electron microscopy. During initial stages of deformation the dislocation density is known to growth along with diminishing of cell sizes. At the same time, there occurs a formation of micro-regions of crystal with some misorientation between them. However, the cell's size remains practically unchanged after reaching $10\div20\%$ strain, Keh *et al.* (1963). Subsequent deformation gives rise to a re-orientation of these micro-

regions. Thus, along with dislocation mechanisms of the re-orientation, rotational deformation modes may play a distinct role already during initial deformational stages.

The orientation (110)[001] is factually opposite for the (001)[110] orientation, and its behaviour at plastic deformation is rather different. At initial deformation stages the active slip systems are the same as for the (001)[110] orientation : (112)[11$\bar{1}$] and (11$\bar{2}$)[111]. Unlike the (001)[110] crystal, the (110)[001] orientation is not stable because these slip systems tend to rotate the crystal in opposite directions around the [$\bar{1}$10] axis. Again, as a result of spreading of the initial orientation, only one after above mentioned slip systems acts at higher strains in a region of the crystal with orientation deflected from initial one. This may result in preferred formation of dislocations with a given sign and, hence, in activation of some process of self-organization. And finally, either microbands or some other structures may emerge. It is of primary interest to study a specific type of such elements. However, there is a difference compared with the case of the (001)[110]-oriented crystal, since the Schmid factor of this slip system will drop with approaching the stable position. Besides that, additional slip systems become active at higher strain. We emphasise that the existence of a specific type of structure that accommodates the misorientation between symmetric orientations is a necessary condition for deformation of crystal with the (110)[001] orientation.

CONCLUSIONS

The combined analysis of microstructure, texture and deformation mechanisms turns out to be very fruitful in the study of plastic deformation in BCC single crystals. Computer simulation shows that both specific microstructure elements and transition texture component must develop if a split into symmetric components occurs during plastic deformation. The nature of the development of such a component may incorporate disclinational features. Presented results may be used for further extension of current models of plastic deformation.

References

Carpay, F. M. A., Mahajan, S., Chin, G. Y. and Rubin, J. J. (1977). *Acta Metall.*, **25**, 149.
De Wit, R. (1972). *J. Phys. Ser.* C. **5**, 529.
Divinski, S. V. and Dnieprenko, V. N. (1993). Texture and Microstructure, **21**, 251.
Divinski, S. V. and Dnieprenko, V. N. (1994). *Proc. of 15th Riso International Symposium on Material Science*, Roskild, Denmark, Sept. 1994. Ed. S. I. Andersen, p. 299.
Dnieprenko, V. N., Larikov, L. N. and Stoyanova, E. N. (1982). *Metallofizika*, **4**, 58.
Dnieprenko, V. N. and Divinski, S. V. (1993). *Texture and Microstructure*, **22**, 73; 169.
Dnieprenko, V. N. (1994). Proc. of ICOTOM-10, Clausthal, Germany, September 1993, *Materials Science Forum*, **157–162**, 1777.
Dunn, C. G. (1954). *Acta Metall.*, **2**, 173.
Hu, H. (1962). *Acta Metall.*, **10**, 1112.
Hu, H. (1963). In *Recovery and Recrystallization of Metals*. Interscience, New York, 311.
Keh, A. S. and Weissmann, S. (1963) in *Electron Microscopy and Strength of Crystals*. Interscience, New York, 231.
Leffers, T. (1968a). *Phys. Stat. Sol.* **25**, 337.
Leffers, T. (1968b). Riso Rep. No. 184.
Li, J. C. M. and Gilman, J. J. (1970). *J. Appl. Phys.*, **41**, 4248.
Romanov, A. E. and Vladimirov, V. I. (1983). *Phys. Stat. Sol.*, **78**, 11.
Rybin, V. V. (1986). *High Plastic Strains and Fracture of Metals*. Metallurgika, Moscow. (*In Russian*).
Takeuchi, T. (1970). *J. Phys. Soc. Jap.* **29**, 291.

Takeuchi, T. (1980). *Scripta Metal.* **14**, 183.
Trefilov, V. I., Mil'man, Yu, V. and Firstov, S. A. (1975). *Physical Basis of Strength of High-Melting-Point Metals.* Naukova Dumka, Kiev. (*In Russian*).
Vandermeer, R. A. and McHarque, C. J. (1964). *Trans. Met. Soc. AIME*, **230**, 667.
Vladimirov, V. I. and Romanov, A. E. (1986). *Disclinations in Crystals.* Nauka, Leningrad. (*In Russian*).
Walter, J. L. and Koch, E. F. (1962). *Acta Metall.*, **10**, 1059.
Walter, J. L. and Koch, E. F. (1965). *Trans. AIME*, **233**, 1209.
Zolotarevsky, N. Yu., Rybin, V. V. and Zhukovsky, I. M. (1989). *Fizika Metallov i Metallovedenie*, **67**, 221.